The Journal of Experimental Biology 215, 1031-1039

doi:10.1242/jeb.060145

REVIEW

The role of structured stirring and mixing on gamete dispersal and aggregation in broadcast spawning

John P. Crimaldi
University of Colorado, Boulder, CO 80309, USA
crimaldi@colorado.edu

Accepted 24 October 2011

Summary

Broadcast-spawning benthic invertebrates synchronously release sperm and eggs from separate locations into the surrounding flow, whereupon the process depends on structured stirring by the flow field (at large scales), and sperm motility and taxis (at small scales) to bring the gametes together. The details of the relevant physical and biological aspects of the problem that result in successful and efficient fertilization are not well understood. This review paper includes relevant work from both the physical and biological communities to synthesize a more complete understanding of the processes that govern fertilization success; the focus is on the role of structured stirring on the dispersal and aggregation of gametes. The review also includes a summary of current trends and approaches for numerical and experimental simulations of broadcast spawning.

Key words: fertilization, gamete dispersal, turbulent mixing.

Introduction

Many benthic invertebrates utilize broadcast spawning as a reproductive strategy. Species using this form of external fertilization are typically sessile (e.g. sea urchins, sea anemones and corals) or are limited in their ability to aggregate by the nature of their chosen habitats or environments. To spawn, adult males and females extrude sperm and ova into the surrounding flow. For fertilization to take place, concentrated parcels of egg and sperm must come into close proximity, and stirring by ambient flow is certain to play an important role in this process. Pioneering work by Denny (Denny, 1988) on the effect of flow on fertilization success showed that models based on the time-averaged gamete plumes downstream of adults strongly under-predict measured fertilization rates, suggesting that instantaneous stirring and mixing processes are important. Unfortunately, the physical and biological factors that govern fertilization success are not well understood in a holistic sense, and there is poor integration between the physical and biological research communities on the topic. This review paper includes relevant work from both the physical and biological communities to synthesize a more complete understanding of the processes that govern fertilization success. There is a strong focus on research from the fluid mechanics community that, although not based on broadcast spawning, may be relevant to its understanding. The paper begins with a discussion of the biological aspects of the broadcast spawning process. This sets the stage for the ensuing discussion of physical processes in the fluid flow that may enhance fertilization success *via* the aggregation of gametes. By necessity, this entails a discussion of the mechanics of stirring and mixing of scalar quantities such as eggs and sperm. The paper concludes with a summary of current numerical and experimental simulations of broadcast spawning.

Biological aspects of the problem

Many species of sessile benthic marine invertebrates reproduce sexually *via* broadcast spawning (e.g. Levitan, 1995; Denny and Gaylord, 2010). In particular, approximately three-quarters of hermatypic (reef-building) corals utilize the strategy. The worldwide demise of coral reefs and subsequent calls for dramatic reassessment of reef management practices (e.g. Bellwood et al., 2004) highlight the necessity of understanding the physical–biological interactions that govern coral reproduction.

A variety of physical, chemical and biological factors affect the fertilization success of corals and other marine benthic invertebrate broadcast spawners. The importance of adult aggregation and distribution has been shown in the field (Pennington, 1985; Levitan et al., 1992; Atkinson and Yund, 1996; Coma and Lasker, 1997; Levitan, 2002; Levitan, 2005a) and with analytical models (Denny et al., 1992; Levitan and Young, 1995; Claereboudt, 1999; Lauzon-Guay and Scheibling, 2007). Adult synchronization of gamete release increases the likelihood of contact between egg and sperm, and mitigates deleterious effects of sperm aging (Giese and Pearse, 1974; Levitan et al., 1991; Levitan, 1995; Lauzon-Guay and Scheibling, 2007). Fertilization success is also influenced by the temporal dynamics of gamete release (e.g. Benzie, 1994), the individual reproductive output and the collective ratio of sperm and ova (Yund, 2000; Levitan, 2005b). Once released into the water column, sperm and ova may coalesce as a result of passive transport by turbulence, or by active sperm swimming. Models and experiments suggest that a combination of large, pheromone-producing eggs and small, motile sperm increases gamete encounter rates (Dusenbery, 2000; Dusenbery, 2002; Podolsky, 2001; Podolsky, 2002). Turbulent stirring and mixing produces long-term dilution of gamete concentrations (Csanady, 1973; Denny et al., 1992), but the dilution may be mitigated by releasing gametes in a viscous matrix (Thomas, 1994a; Marshall, 2002; Yund and Meidel, 2003), or through gamete sequestration in surge channels (Denny et al., 1992) and tide pools (Pearson and Brawley, 1996). Once a sperm–ova collision takes place, a variety of factors including sperm age, compatibility and the jelly coat thickness of the egg determine

whether the collision will lead to successful fertilization (Levitan, 1995). Even if fertilization does take place, other factors, including polyspermy (Byrd and Collins, 1975; Styan, 1998) and excessive hydrodynamic shear (Denny et al., 2002; Gaylord, 2008), can impede the proper development of the zygote.

Despite the complexities of the process, the average fertilization success measured in field studies for a wide range of taxa is rarely less than 5%, and often exceeds 90%; when the nearest spawning male is closer than 1 m away, the fertilization success is typically greater than 50% (e.g. Babcock et al., 1994; Benzie et al., 1994; Eckman, 1996; Yund, 2000; Marshall, 2002). Field observations also show high variability in local fertilization rates, with marked variation even on scales of seconds and centimeters (Coma and Lasker, 1997). This observed variation suggests that the instantaneous turbulent structure of the gamete fields is fundamental to the process.

Modern efforts to model broadcast spawning fertilization rates are based on the fertilization kinetics model developed by Vogel et al. (Vogel et al., 1982) or extensions of it that incorporate effects of polyspermy (Styan, 1998; Styan and Butler, 2000; Millar and Anderson, 2003), gamete covariance (Luttikhuizen et al., 2004) or non-complete fertilization (Hodgson et al., 2007). In all cases, fertilization is treated as a bimolecular reaction between two scalar species (egg and sperm). The likelihood of an individual egg being fertilized is dependent on sperm concentration, and the resulting dimensional fertilization rate is $\phi C_E C_S$, where C_E and C_S are 'virgin' egg and sperm concentrations, respectively, and ϕ is a rate constant (Denny and Shibata, 1989; Crimaldi and Browning, 2004; Crimaldi et al., 2006; Crimaldi et al., 2008). Average gamete concentrations are typically calculated using an analytical model for a time-averaged plume (Csanady, 1973), or a modified version of it (e.g. Babcock et al., 1994; Lauzon-Guay and Scheibling, 2007). This approach requires the adoption of an effective turbulent diffusivity that sets the spreading rate of the resulting Gaussian plume. This combination of models for fertilization kinetics and mean plume concentrations forms the basis for a range of analyses of fertilization success of free-spawning invertebrates (e.g. Denny, 1988; Denny and Shibata, 1989; Denny et al., 1992; Babcock et al., 1994; Levitan and Young, 1995; Metaxas et al., 2002; Lauzon-Guay and Scheibling, 2007). None of these studies, however, consider the role of instantaneous structure of the gamete plumes.

Broadcast spawners typically release gametes in a viscous matrix that may resist dilution (Thomas, 1994a; Marshall, 2002), form clumps or strings that can cling to adults (Picken and Allan, 1983; McEuen, 1988; Thomas, 1994a; Yund and Meidel, 2003), or prolong gamete viability (Levitan et al., 1991; Meidel and Yund, 2001). The rheology of the gamete matrix is typically non-Newtonian and exhibits shear-thinning properties that facilitate extrusion through the gonoduct (Thomas, 1994a). Shear-thinning fluids are known to disperse and mix differently than Newtonian fluids (e.g. Niederkorn and Ottino, 1994), but the role of this rheological factor on gamete distribution and fertilization success is unknown.

Gamete buoyancy varies between species, influences gamete distribution within the water column, and may increase the chances of intraspecific egg and sperm contact (Thomas, 1994b). Sea urchin gametes are typically negatively buoyant (Thomas, 1994a; Yund and Meidel, 2003), with larger eggs sinking faster (Levitan, 2006), whereas most mass-spawning coral species have highly buoyant gamete bundles (Babcock et al., 1986), compressing gamete interactions into two dimensions at the sea surface (Oliver and Willis, 1987; Moore, 2003). Floating particles are known to cluster because of effects of turbulence (Schumacher and Eckhardt, 2002; Cressman et al., 2004), surface waves (Denissenko et al., 2006; Lukaschuk et al., 2006), surface tension (Singh and Joseph, 2005) or wind-induced Langmuir circulations (Larson, 1992; Thorpe, 2004), but the quantitative effect of these clustering mechanisms on gamete distribution and fertilization success is unknown.

It is generally thought (Vogel et al., 1982) that increases in egg size enhance sperm collision frequency and resulting fertilization rates, although the effect may not be present in all species (e.g. Styan et al., 2005). Extracellular structures surrounding many marine invertebrate eggs that increase their effective size might be an evolutionary response to sperm limitation (Levitan, 1993; Farley and Levitan, 2001). However, very little is known about the hydrodynamic effect of egg size on gamete coalescence and fertilization rates.

Sperm chemotaxis has been documented in several phyla (Miller, 1985; Miller, 1997), but the demonstrated attraction distance is small (100–200 μm). Sperm in proximity to eggs swim faster and orient towards the egg surface (Riffell and Zimmer, 2007). Sperm swimming velocities for several benthic invertebrates have been measured to be in the range of 0.05 to 0.3 mm s^{-1} (Gray, 1955; Levitan et al., 1991; Levitan, 1993; Riffell and Zimmer, 2007). Because the separation between spawning adults is on the scale of centimeters or meters, and the velocity fluctuations in typical turbulent benthic flows are on the scale of 0.01 to 0.1 m s^{-1} (Denny, 1988), it is likely that large-scale sperm motion is almost entirely passive (Eckman, 1996), and it has been suggested that the action of sperm swimming and chemotaxis is unlikely to substantially increase egg–sperm collisions (Levitan, 1995). However, if external clustering mechanisms bring sperm and eggs into close proximity, sperm swimming and taxis might significantly increase contact rates (Jantzen et al., 2001).

Physical aggregation processes

The physical environment

Broadcast spawning by benthic invertebrates occurs, at least initially, in the boundary layer flow that forms a transition between the bulk water column and the bed. Benthic boundary layers form in a broad range of hydrodynamic conditions, but most flow over and around significant bed topography (Boudreau and Jørgensen, 2001), are subject to the oscillatory effect of surface waves (Reidenbach et al., 2006) and are at least weakly turbulent (Denny, 1988). Surface waves produce dramatic changes in benthic boundary layer flows (Grant and Madsen, 1979), altering turbulence structure and intensity. The flow environment in spawning regions is also influenced by unsteady vortex shedding in wakes behind obstacles (Ferrier et al., 1996; Guichard and Bourget, 1998). The obstacles can be the animals themselves (e.g. urchins or coral heads) or local bed topography.

Little is known about the direct effect of structured flow and turbulence on gamete coalescence and dispersion at instantaneous time scales. Laboratory studies in a simple sheared flow between rotating cylinders (Mead and Denny, 1995; Denny et al., 2002) show a modest increase in average fertilization rates at moderate turbulence levels (presumably due to increased contact rates), followed by a more dramatic fertilization decrease at higher turbulence levels (perhaps due to shear-induced damage to gametes). However, these experiments were performed at a scale that is too small to properly simulate the complexity of benthic turbulence (Sanford, 1997). To learn more about the physical processes in turbulence that might influence fertilization, therefore, we turn to studies of related topics dealing with turbulent stirring and mixing.

Fundamentals of scalar stirring and mixing

We begin with a brief overview of the physical processes responsible for stirring, mixing and reaction of chemicals or particles [for more details, see Moore and Crimaldi (Moore and Crimaldi, 2004)]. Chemicals (e.g. odors and nutrients) or small particles (e.g. eggs and sperm) transported by a flow are generically called scalars; the spatial distribution of the concentration of these scalars is called a scalar field. Scalars are transported in a fluid flow by two processes: advection and dispersion. Advection is the macroscopic transport by the bulk flow. Dispersion is any process that causes the scalar field to spread, typically from regions of high scalar concentration to regions of low concentration. Dispersion results from the combined effects of one or more of the following processes: spreading at large scales due to shear in the mean velocity field (shear dispersion), intermingling of fluid parcels at intermediate scales by local fluid motion (stirring), and actual dilution of the scalar field at molecular scales by Brownian motion (diffusive mixing). Spatial structure in the velocity field deforms (stirs) the scalar field into elongated thin filaments (e.g. Crimaldi and Koseff, 2006); this action does not directly dilute the scalar field, but indirectly promotes diffusion and dilution by enhancing the interfacial area between intermingled fluid parcels, and sharpening scalar gradients across the filaments.

Molecular diffusion eradicates spatial variation (gradients) in the scalar field *via* a net flux of scalar mass in the direction of decreasing concentration. This process is described by the Fickian relationship:

$$\vec{\mathbf{q}} = -D_{\mathrm{m}}\nabla C\,, \tag{1}$$

where a diffusive scalar flux $\vec{\mathbf{q}}$ is driven in the direction of decreasing concentration (given by $-\nabla C$). The propensity of a given scalar to diffuse by molecular processes in a given fluid is quantified by the molecular diffusivity D_{m}. The molecular diffusivity of relevant scalars in aquatic environments is small (of the order of $10^{-9}\,\mathrm{m^2\,s^{-1}}$ for solutes, and even lower for discrete particles), so the effect of diffusion is prevalent only when the change in scalar concentration is large over a small distance (large ∇C).

The Péclet number describes the importance of molecular diffusion relative to the advective strength of the flow. For a flow with mean velocity U, the time required to advect a small particle over a distance L is $t_{\mathrm{a}}=L/U$. The time for a particle to diffuse the same distance scales as $t_{\mathrm{d}}=L^2/D_{\mathrm{m}}$. The Péclet number is the ratio of these two times, given by:

$$Pe = \frac{t_{\mathrm{a}}}{t_{\mathrm{d}}} = \frac{UL}{D_{\mathrm{m}}}\,. \tag{2}$$

When $Pe\ll 1$ (typical for extremely low velocities or small spatial scales), diffusive processes are important. When $Pe\gg 1$, advection is the dominant process, and molecular diffusion is unimportant at all but the smallest scales.

The nature of the flow field (e.g. a laminar wake or a turbulent boundary layer) depends on the relative amount of energy in the flow. The Reynolds number quantifies this characteristic *via* the relationship:

$$Re = \frac{UL}{\nu}\,, \tag{3}$$

where ν is the kinematic viscosity of the fluid (which is the molecular diffusivity for momentum in the fluid). As a general rule, as Reynolds number increases, flow fields tend to be more complex, have more energetic stirring mechanisms over a broader range of spatial scales, and are likely to become turbulent.

The equations for Péclet number and Reynolds number have similar forms and analogous interpretations. The Péclet number compares the rate of advective scalar transport with the rate of smearing (smoothing or eradication by diffusion) of gradients and spatial structures in the scalar field. The Reynolds number compares the rate of advective transport of momentum with the rate of molecular smearing of velocity gradients (spatial structures in the velocity field). The two numbers are related through the Schmidt number, defined as the ratio of *Pe* to *Re*:

$$Sc = \frac{Pe}{Re} = \frac{\nu}{D_{\mathrm{m}}}\,, \tag{4}$$

which ends up being simply the ratio of the molecular diffusivities of momentum and the scalar. Typical aquatic scalars have a Schmidt number on the order of 10^3 for solutes, and even higher for particles, and are therefore referred to as weakly diffusive (relative to the diffusion of momentum). Note that only two of the three parameters *Pe*, *Re* and *Sc* are required to specify a flow condition; the third parameter can be calculated from the other two.

If a flow contains two scalars (denoted *A* and *B*) that react with each other, the dimensional rate at which scalar mass is removed from the flow by the reaction (and converted to reaction product) is given by:

$$R = \phi C_{\mathrm{A}}^{m} C_{\mathrm{B}}^{n}\,, \tag{5}$$

where ϕ is the dimensional reaction rate constant, and $p=m+n$ is the total reaction order. Following the methodology used to define the Péclet number above, the relative rate at which the reaction depletes reactant from the system can be described as the ratio of the diffusive time scale t_{d} to the reactive time scale $t_{\mathrm{r}}=L^2/\phi M$, where M is the total scalar mass. The resulting ratio, called a Damköhler number, is:

$$Da = \frac{t_{\mathrm{d}}}{t_{\mathrm{r}}} = \frac{\phi M}{D_{\mathrm{m}}}\,. \tag{6}$$

When $Da\ll 1$, reactions proceed slowly relative to the rate of diffusive mixing, and the rate at which reactant mass is depleted from the system is negligible. When $Da\gg 1$, the reaction removes the scalar mass on contact, leading to the formation of reactive fronts.

The role of instantaneous stirring

One of the classic paradigms of turbulent mixing is that turbulence produces rapid dilution of introduced scalars. The pioneering work by Richardson (Richardson, 1926) on relative turbulent dispersion predicts that the average distance between two closely spaced passive particles grows exponentially in time as $t^{3/2}$. This dispersion, and associated dilution, might suggest that flow-induced stirring and mixing is detrimental to broadcast spawning fertilization success. To get a better sense of the true role of flow processes, it is necessary to consider the instantaneous (as opposed to average) effect of stirring. Recent numerical studies, for example, show that the Richardson's particle separation is produced by rare, extreme events, and the majority of initially close pairs are not dispersed by the flow (e.g. Sokolov, 1999). Thus, two gametes that are brought into close proximity by turbulent stirring (achieving contact perhaps *via* sperm taxis) might spend sufficient time in close contact for fertilization to occur before a rare event causes them to dramatically separate. Furthermore, there are many

mechanisms in structured flows that produce local aggregation (rather than dispersion and dilution) of scalar particles. These mechanisms could promote local coalescence of gametes at intermediate time scales (resulting in dramatically enhanced fertilization rates), even though the average effect of the flow at longer time scales produces dilution.

Coagulation of particles is an important mechanism for mass transport in the ocean (reviewed by Jackson and Burd, 1998) and in benthic boundary layers (Hill and Nowell, 1995; Hill and McCave, 2001). Enhancement of particle encounter rates by turbulence has been shown in the laboratory for synthetic particles (Hill et al., 1992) and with modeling approaches for plankton or other marine particles (Squires and Yamazaki, 1995; Rothschild and Osborn, 1988; Lewis, 2003). Surface waves produce clustering of buoyant particles, with the effect increasing as the square of wave amplitude (Denissenko et al., 2006; Lukaschuk et al., 2006). Unsteady wakes (e.g. Kármán vortex streets) behind flow obstacles serve as effective reactors for bimolecular reactions (Kastrinakis and Nychas, 1998; Toroczkai et al., 1998; Karolyi et al., 1999). Obstacle wakes alter scalar structure (Rehab et al., 2001) and produce clustering of inertial particles (Tang et al., 1992; Helgesen and Matteson, 1994).

Particles that are sufficiently small and neutrally buoyant move passively with the ambient flow. As particles become larger or non-neutrally buoyant, they act as if they have inertia relative to the local flow. These inertial effects cause the temporal response characteristics of large or non-neutrally buoyant particles to differ from those of the surrounding fluid (or of dissolved scalars in the fluid). Squires and Eaton (Squires and Eaton, 1991) used direct numerical simulations to show that dense particles collect preferentially in regions of low vorticity and high strain rate. Related experiments (Tang et al., 1992; Crowe et al., 1995) show that particles within intermediate size ranges are focused along the boundaries of coherent vortex structures. Turbulence has been shown to increase collision rates between inertial particles (Reade and Collins, 2000), and to segregate particles with differing densities (Reigada et al., 2001). Even neutrally buoyant particles (of finite size) move in a non-passive manner because of particle–flow interactions (Maxey, 1990), and aggregate near vortex cores (Babiano et al., 2000). Nonetheless, neutrally buoyant particles that are sufficiently small are often assumed to move passively, without disturbing the ambient flow. In this case, the turbulent particle advection problem can be approximated by using dissolved passive scalars (e.g. fluorescent dye) as surrogates for the particles. This is convenient, because a large body of literature exists for the turbulent mixing of passive scalars (reviewed by Warhaft, 2000).

Buoyancy can also cause aggregation of particles on the free surface of the flow. Buoyant gametes follow pathlines on the free surface of the turbulent flow in which they were released. The transport and coalescence of floating gametes is fundamentally different from sub-surface transport because of differences in the nature of free-surface turbulence. The kinematic boundary condition at the free surface (vertical velocities=0) produces a blockage layer that increases horizontal turbulence intensities at the expense of those in the vertical direction; the dynamic boundary condition at the surface (stress=0) results in a thinner surface layer characterized by fast variations of the horizontal vorticity components (Shen et al., 1999). The surface flow (and the path of particles following it) is compressible (meaning that particles can aggregate) even when the underlying flow is incompressible. This results in regions of surface flow convergence (corresponding to downwelling in the bulk flow) and divergence (corresponding to upwelling) (Kumar et al., 1998). The inability of floating particles to enter the bulk flow in surface convergence zones therefore leads to coalescence. The extent to which the surface flow deviates from incompressibility is quantified by the compressibility coefficient:

$$C = \frac{\left\langle (\nabla_s \cdot \vec{u}_s)^2 \right\rangle}{\left\langle (\nabla_s \vec{u}_s)^2 \right\rangle} , \quad (7)$$

where the subscript s denotes that only derivatives and velocities in the surface plane are computed. This quantity is found to be close to 1/2, both experimentally (Goldburg et al., 2001) and numerically (Eckhardt and Schumacher, 2001). Coalescence of buoyant particles has been demonstrated experimentally (Cressman et al., 2004; Bandi et al., 2008) and numerically (Eckhardt and Schumacher, 2001; Schumacher and Eckhardt, 2002; Boffetta et al., 2004; Ducasse and Pumir, 2008). However, the effect of turbulence on distributed (non-point) scalars on the free surface has not been studied, and the quantitative effect of these clustering mechanisms on initially distant scalars and subsequent fertilization success is unknown.

Studies of the instantaneous processes governing turbulent scalar mixing are complicated by the fact that turbulence is chaotic, exhibiting an acute sensitivity to changes in initial conditions (Pope, 2000). Turbulence first stirs scalars into thin filaments (Eckart, 1948; Garrett, 1983), enhancing local scalar gradients and increasing the interfacial area of the scalar through processes of stretching and folding (Ottino, 1989; Hinch, 1999), leading to increased mixing by molecular diffusion. A blob of a weakly diffusive scalar is stirred into well-defined filaments, with alternating striations of marked and unmarked fluid; the striation thickness decreases with time, but the low molecular diffusivity initially discourages dilution at the molecular scale. Paradoxically, turbulent stirring initially promotes scalar heterogeneity (or ‘patchiness’) (e.g. Abraham, 1998), but this introduced heterogeneity enhances gradients in the scalar field, thereby enhancing scalar diffusion, ultimately destroying the original scalar heterogeneity.

The aggregate effect of instantaneous turbulent stirring and mixing is often modeled using an enhanced diffusion coefficient called an eddy viscosity (for diffusion momentum) or an eddy diffusivity (for diffusion scalars). This approach assumes that the complex actions of instantaneous stirring and mixing have the same effect (in a time-averaged sense) as a simple Fickian diffusion process (with a diffusion coefficient much larger than the molecular value). Although this method is sometimes satisfactory, it can fail spectacularly. For example, in the broadcast spawning problem, field measurements of fertilization rates are rarely less than 5%, and are often as high as 90% (Eckman, 1996; Pennington, 1985; Yund, 2000). However, numerical modeling using a turbulent eddy diffusivity predicts fertilization rates of only 0.01–1% because of the strong time-average turbulent dilution of the gametes (Denny and Shibata, 1989).

Many studies (e.g. Edouard et al., 1996; Ottino, 1994) have demonstrated that the instantaneous details of advective transport (not captured by the eddy diffusivity approach) can enhance reactions rates for scalars that are initially in contact and share a material interface. In broadcast spawning, however, egg and sperm are typically released from separate locations, and the ambient fluid that separates them initially acts as a barrier to fertilization. It is likely that turbulence and structure stirring produce similar reaction enhancements in processes such as broadcast spawning where the reactive scalars are initially distant (Crimaldi and Browning, 2004).

Fertilization can be modeled as a bimolecular reaction between two scalars, egg and sperm (Vogel et al., 1982; Styan, 1998). Instantaneous gamete concentrations in unsteady flows are governed by a coupled pair of reactive advection-diffusion equations that can be expressed nondimensionally as (Crimaldi et al., 2008):

$$\frac{\partial C_{\mathrm{E}}}{\partial t} = -Pe\ \vec{u}\cdot\nabla C_{\mathrm{E}} + \nabla^2 C_{\mathrm{E}} - \Theta\ , \tag{8}$$

and

$$\frac{\partial C_{\mathrm{S}}}{\partial t} = -Pe\ \vec{u}\cdot\nabla C_{\mathrm{S}} + \nabla^2 C_{\mathrm{S}} - \Theta\ , \tag{9}$$

where $\Theta=DaC_{\mathrm{E}}C_{\mathrm{S}}$ is the nondimensional fertilization rate and Da is the Damköhler number (a nondimensional version of ϕ). The Péclet number, Pe, describes the relative advective strength of the flow, and can be expressed as the product of the Reynolds number and Schmidt number: $Pe=Re\times Sc$. Using a standard Reynolds decomposition (e.g. Adrian et al., 2000), the local gamete concentrations can be decomposed into the sum of a mean component (denoted by an overbar) and a fluctuating component relative to the mean (denoted by a prime):

$$C_{\mathrm{E}}(t) = \overline{C}_{\mathrm{E}} + C'_{\mathrm{E}}(t)\ , \tag{10}$$

and

$$C_{\mathrm{S}}(t) = \overline{C}_{\mathrm{S}} + C'_{\mathrm{S}}(t)\ . \tag{11}$$

By substituting these decompositions into the expression for Θ and then averaging, the averaged value (inclusive of instantaneous physics) of the normalized fertilization rate Θ/Da is then (Crimaldi et al., 2006):

$$\overline{C_{\mathrm{E}}(t)C_{\mathrm{S}}(t)} = \overline{C_{\mathrm{E}}C_{\mathrm{S}}} + \overline{C'_{\mathrm{E}}(t)C'_{\mathrm{S}}(t)}\ , \tag{12}$$

where the first term on the right-hand side is simply the product of the average concentrations, and the second term is the correlation between the fluctuating concentrations. Positive contributions to the correlation term would be associated with spatial coalescence of the initially distant scalars as a result of structured stirring. These contributions would not be captured by time-averaged models that use an eddy diffusivity as an average metric for the effect of turbulent stirring. Recent work, described below, shows that these contributions may indeed by large, suggesting that instantaneous stirring and mixing processes are crucial to an understanding of broadcast spawning success.

Numerical and laboratory studies

Recent numerical simulations (Crimaldi and Browning, 2004; Crimaldi et al., 2006; Crimaldi et al., 2008) demonstrate the ability of structured flow fields to impart spatial correlations onto a pair of initially distant scalars (surrogates for egg and sperm), thereby enhancing reaction or fertilization rates. This coalescence occurs even though each scalar has no knowledge of the other (there was no modeled sperm motility or taxis). Instead, the structure of the velocity field that is shared by the two scalars (even though they are initially distant) is responsible for the coalescence.

One of the simplest structured flow fields is that of a single two-dimensional vortex. This flow has an analytical description that facilitates modeling, and it is easily created in a laboratory. The flow is a good model system in that it provides insight into more complex flows that consist of multiple, interacting vortices. For example, laminar wakes behind obstacles consist of a sequence of vortices shed periodically from either side of the obstacle. Turbulent flows consist of a range of vortices (often termed eddies in that context) that interact in a chaotic manner. To build a process-level understanding of these more complex flows, it is useful to study the underlying building block consisting of a single vortex.

If two initially separate parcels of egg and sperm are located in the vicinity of a structured vortex flow, the vortex imposes a shared spiral structure on the gamete filaments. A simple analytical model demonstrates this process (Fig. 1). Parcels of egg (within the

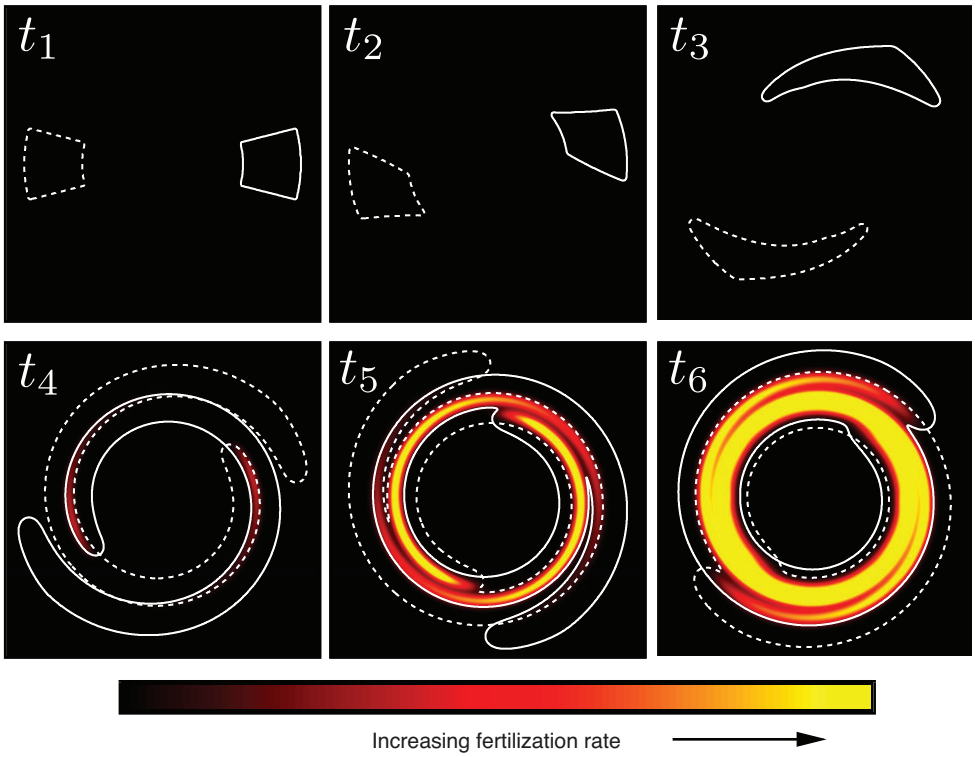

Fig. 1. Analytical model of scalar stirring by a single point vortex. In the initial condition (t_1), separate parcels of egg (solid line) and sperm (dashed line) are stirred and strained by the vortex flow (t_2 through t_6). The egg and sperm parcels assume the circular symmetry of the flow, and radial diffusion causes the overlap between the gamete sets. The resulting fertilization rate is shown in red and yellow. Without the vortex stirring, relatively little fertilization would take place.

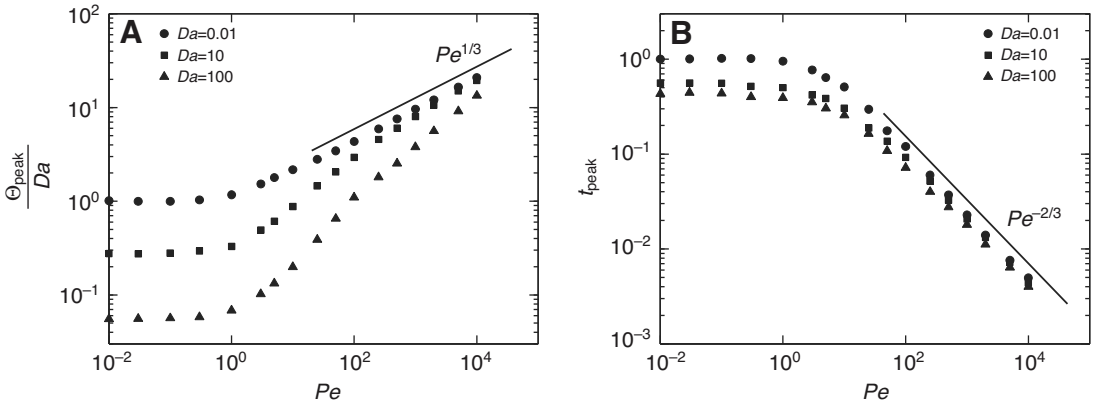

Fig. 2. (A) Normalized peak fertilization rate (Θ_{peak}/Da, where Da is the Damköhler number) and (B) nondimensional time to peak fertilization rate (t_{peak}) as a function of Péclet number (Pe) for three values of Da. Results of the numerical simulation are shown as symbols, and the resulting Pe scaling is shown as a solid line. Reprinted by permission from Crimaldi et al. (Crimaldi et al., 2008).

boundary shown by the solid line) and sperm (dashed line) are placed in a flow field consisting of a single point vortex. The vortex flow moves in circles about its center, with the magnitude of the velocity decaying inversely with distance from the center. This decay is typical of the far-field behavior for all real vortices. Because the portions of the egg and sperm parcels near the center are moving faster, the parcels begin to strain and distort as they advect around the vortex center. This strains the parcels into long, thin filaments, enhancing scalar gradients (and hence diffusion) in the radial direction. Quite quickly, the parcels assume a spiral geometry that is dictated by the flow field. The scalar fields become correlated over time, and begin to overlap. As concentrations of egg and sperm begin to coalesce, fertilization rates grow rapidly until they reach a peak. Beyond that time (corresponding to times greater than that shown in Fig. 1), radial diffusion spreads the gametes beyond the scope of the vortex, and the dilution results in lowered fertilization rates. Note that without the vortex field, only diffusion (and sperm motility) could bring the gametes together, resulting in dramatically lower fertilization rates.

A numerical model was used to quantify the fertilization enhancement rate caused by a single vortex as a function of Péclet number (Pe, nondimensional stirring rate) and Damköhler number (Da, nondimensional reaction rate). Here we consider the peak fertilization rate Θ_{peak} normalized by Da; the resulting ratio is equivalent to the product of co-occuring gamete concentrations $C_E C_S$. This is plotted as a function of Pe for several values of Da (Fig. 2A). The constant fertilization rates for $Pe<<1$ correspond to the case where the vortex stirring is inconsequential and only diffusion produces scalar overlap. As Pe increases, the stirring increases in strength and fertilization is enhanced. When $Pe>>1$, the fertilization rate grows exponentially as $Pe^{1/3}$. Thus, the stronger the vortex, the greater the enhancement. For high Péclet numbers typical of the ocean, the resulting fertilization enhancement could be several orders of magnitude relative to the non-stirred case.

The vortex stirring also shortens the time required for peak fertilization to occur (Fig. 2B). This is relevant when gamete viability is considered. The time t_{peak} is the time to peak fertilization, normalized by the time to peak for pure diffusion. For $Pe<<1$ (no stirring), the values of $Pe<<1$ asymptote to values near unity. For $Pe>>1$, t_{peak} decreases exponentially as $Pe^{-2/3}$.

The obvious question is, how do these idealized single-vortex model results scale up to more realistic flows? There are, at this point, no concrete answers to this question, but there are some strong hints that the coalescence mechanisms are similar in more complex flows. Fig. 3 shows the results from a numerical study with 50 interacting vortices (black crosses) stirring and straining initially separate discrete blobs of egg (red) and sperm (blue). In this case, the flow field is chaotic, with complex stirring processes.

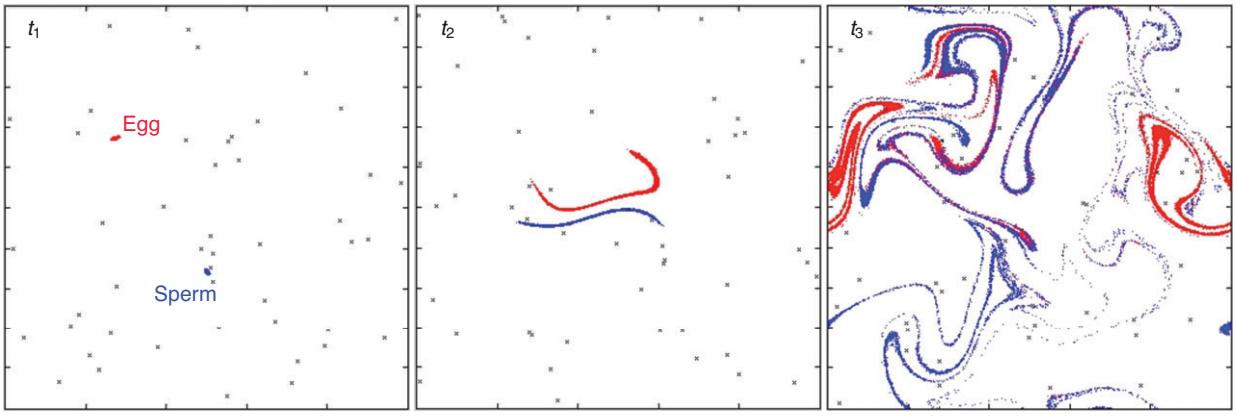

Fig. 3. Spatial coalescence of packets of egg (red) and sperm (blue) in a two-dimensional pseudo-turbulent flow field consisting of multiple, interacting vortices. Image courtesy of Jillian Cadwell.

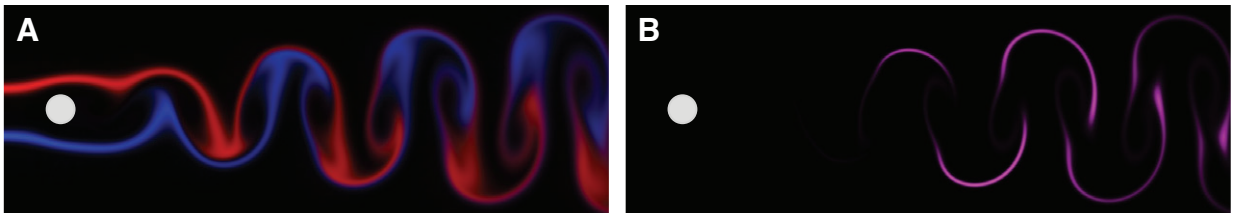

Fig. 4. Numerical simulations of a two-dimensional flow around a round obstacle (white) at a Reynolds number (*Re*) of 100 and a Schmidt number (*Sc*) of 10 showing (A) dispersion of egg (red) and sperm (blue), and (B) local fertilization rate. Compare with experimental results (for a slightly different geometry) for *Sc*=1000 in Fig. 5. Flow is from left to right.

In the simulation shown, the egg and sperm rapidly develop strong spatial correlations, resulting in enhanced fertilization rates. In the parlance of nonlinear dynamics, the regions of filament coalescence correspond to unstable manifolds within the chaotic flow (Ottino, 1989). However, because the flow is chaotic, small changes in the initial conditions produce large changes in the results, and not all simulations produce the large coalescence shown here. Additional work is needed to determine the average effect of these complex instantaneous processes.

Because of the complexity of chaotic turbulent flows, it is useful to also look at simpler (but still realistic) laminar flows consisting of interacting vortices. The unsteady wake behind an obstacle (e.g. a coral head) is an obvious example. Numerical simulations of a two-dimensional flow around a round obstacle (Fig. 4) demonstrate fertilization enhancement mechanisms that appear to be extensions of the simpler processes seen in the single vortex models. For these simulations, a steady stream of egg (red) and sperm (blue) are transported past the obstacle by the mean flow. In the absence of the obstacle, only diffusion and sperm motility could bridge the lateral distance between the gamete streams. But vortices shed off the back of the obstacle produce lateral entrainment, with resulting scalar coalescence in the wake (Fig. 4A). The spatial distribution of the computed fertilization rate (Fig. 4B) shows spiral regions of enhanced fertilization (purple), reminiscent of the structures seen in the single-vortex flow.

Laboratory experiments in a water flume of a similar wake geometry are shown in Fig. 5, where a two-color planar laser-induced fluorescence system (Soltys and Crimaldi, 2010) is used to visualize quantify the scalar fields. Fluorescent dyes are used as high-Schmidt-number surrogates for egg (red) and sperm (blue).

The downstream development of spatial correlations between the gamete sets is obvious, and extremely similar to the numerical simulation shown in Fig. 4 (even though the geometries are slightly different). The advantage of the laboratory approach shown here is that measurements can be made for much more complex and realistic flows (e.g. turbulent boundary layers) than are feasible with numerical simulations. This approach holds significant promise for ultimately understanding and quantifying the role of structured stirring on gamete coalescence and fertilization success in complex flow environments

Conclusions

Time-averaged models of broadcast spawning (including those using an eddy-diffusivity approach to model turbulence) appear destined to dramatically under-predict fertilization rates measured in the field, or even those necessary for species survival. It is likely that the shortcoming in the modeling approach is that the details of the instantaneous stirring and mixing processes are crucial to enhancing the fertilization rate. Although many previous studies have demonstrated the role of stirring on enhanced reactions for reactive scalars that are initially in contact with one another, egg and sperm are released at different locations within a flow, and the role of structured stirring on fertilization rates in this case is not well understood. Numerical simulations of simple vortex flows demonstrate that structure in the velocity field imposes spatial correlations on initially distant parcels of egg and sperm, resulting in enhanced fertilization rates. More complex models suggest that these processes extend to more realistic flows, and laboratory experiments are being developed that may be able to quantify fertilization enhancement it in real three-dimensional turbulent flows.

A variety of biologically relevant details also need further study. The role of gamete buoyancy and the resulting coalescence properties of free-surface flows may help explain the selective benefit for species with buoyant gametes. Sperm motility and taxis has not been included in any of the current models. If physical stirring processes are able to bring weakly diffusive parcels of egg and sperm into close proximity, sperm motility combined with taxis could serve as a ‘directed diffusion’ that selectively bridges the gap to nearby eggs. Finally, the viscous non-Newtonian matrix in which gametes are often secreted may help to resist scalar dilution during the intermediate time scales where structured stirring is in the process of bringing gamete filaments into closer contact.

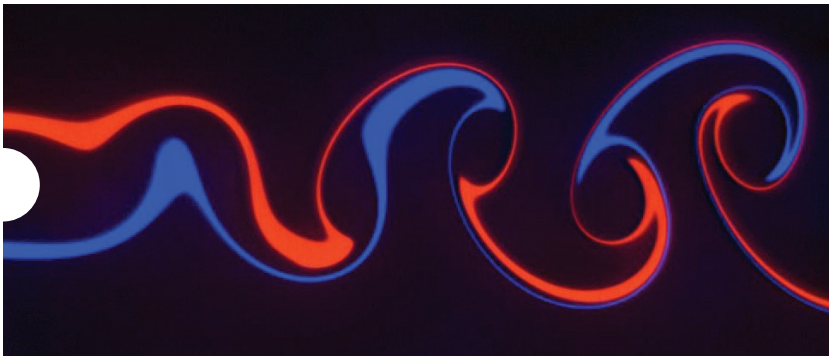

Fig. 5. Laboratory results from a two-color planar laser-induced fluorescence system showing coalescence of surrogate egg (red) and sperm (blue) solutions in the wake of a cylinder for *Re*=100, *Sc*=1000. Half of the cylinder (white) is at the left edge. Flow is from left to right. Image courtesy of Mike Soltys.

This work lies within the broader topic of how spatial structure develops in coupled physical–biological systems. Much of the patchiness that is emblematic of the marine environment is produced by some interaction between physics and biology. For a related study of structure imposed by the interplay between motility and diffusion, see Jackson (Jackson, 2012).

Acknowledgements

The author would like to acknowledge contributions to this manuscript from current and former students Mike Soltys and Dr Jillian Cadwell.

Funding

This work was supported by the National Science Foundation under grant 0849695.

References

Abraham, E. R. (1998). The generation of plankton patchiness by turbulent stirring. *Nature* **391**, 577-580.

Adrian, R. J., Christensen, K. T. and Liu, Z. C. (2000). Analysis and interpretation of instantaneous turbulent velocity fields. *Exp. Fluids* **29**, 275-290.

Atkinson, O. S. and Yund, P. O. (1996). The effect of variation in population density on male fertilization success in a colonial ascidian. *J. Exp. Mar. Biol. Ecol.* **195**, 111-123.

Babcock, R. C., Bull, G. D., Harrison, P. L., Heyward, A. J., Oliver, J. K., Wallace, C. C. and Willis, B. L. (1986). Synchronous spawnings of 105 scleractinian coral species on the Great Barrier Reef. *Mar. Biol.* **90**, 379-394.

Babcock, R. C., Mundy, C. N. and Whitehead, D. (1994). Sperm diffusion models and *in situ* confirmation of long-distance fertilization in the free-spawning asteroid *Acanthaster planci*. *Biol. Bull.* **186**, 17-28.

Babiano, A., Cartwright, J. H. E., Piro, O. and Provenzale, A. (2000). Dynamics of a small neutrally buoyant sphere in a fluid and targeting in Hamiltonian systems. *Phys. Rev. Lett.* **84**, 5764-5767.

Bandi, M. M., Cressman, J. R. and Goldburg, W. I. (2008). Test of the fluctuation relation in Lagrangian turbulence on a free surface. *J. Stat. Phys.* **130**, 27-38.

Bellwood, D. R., Hughes, T. P., Folke, C. and Nystrom, M. (2004). Confronting the coral reef crisis. *Nature* **429**, 827-833.

Benzie, J. A. H., Black, K. P., Moran, P. J. and Dixon, P. (1994). Small-scale dispersion of eggs and sperm of the crown-of-thorns starfish (*Acanthaster planci*) in a shallow coral reef habitat. *Biol. Bull.* **186**, 153-167.

Boffetta, G., Davoudi, J., Eckhardt, B. and Schumacher, J. (2004). Lagrangian tracers on a surface flow: The role of time correlations. *Phys. Rev. Lett.* **93**, 134501.

Boudreau, B. P. and Jørgensen, B. B. (2001). *The Benthic Boundary Layer: Transport Processes and Biogeochemistry*. Oxford, New York: Oxford University Press.

Byrd, E. W., Jr and Collins, F. D. (1975). Absence of fast block to polyspermy in eggs of the sea urchin *Strongylocentrotus purpuratus*. *Nature* **257**, 675-677.

Claereboudt, M. (1999). Fertilization success in spatially distributed populations of benthic free-spawners: a simulation model. *Ecol. Model.* **121**, 221-233.

Coma, R. and Lasker, H. (1997). Effects of spatial distribution and reproductive biology on in situ fertilization rates of a broadcast-spawning invertebrate. *Biol. Bull.* **193**, 20-29.

Cressman, J. R., Davoudi, J., Goldburg, W. I. and Schumacher, J. (2004). Eulerian and Lagrangian studies in surface flow turbulence. *New J. Phys.* **6**, 53.

Crimaldi, J. P. and Browning, H. S. (2004). A proposed mechanism for turbulent enhancement of broadcast spawning efficiency. *J. Mar. Syst.* **49**, 3-18.

Crimaldi, J. P. and Koseff, J. R. (2006). Structure of turbulent plumes from a momentumless source in a smooth bed. *Environ. Fluid Mech.* **6**, 573-592.

Crimaldi, J. P., Hartford, J. R. and Weiss, J. B. (2006). Reaction enhancement of point sources due to vortex stirring. *Phys. Rev. E* **74**, 016307.

Crimaldi, J. P., Cadwell, J. R. and Weiss, J. B. (2008). Reaction enhancement of isolated scalars by vortex stirring. *Phys. Fluids* **20**, 073605.

Crowe, C. T., Troutt, T. R., Chung, J. N., Davis, R. W. and Moore, E. F. (1995). A turbulent flow without particle mixing. *Aerosol Sci. Technol.* **22**, 135-138.

Csanady, G. T. (1973). *Turbulent Diffusion in the Environment*. Boston, MA: Reidel.

Denissenko, P., Falkovich, G. and Lukaschuk, S. (2006). How waves affect the distribution of particles that float on a liquid surface. *Phys. Rev. Lett.* **97**, 244501.

Denny, M. W. (1988). *Biology and the Mechanics of the Wave-swept Environment*. Princeton, NJ: Princeton University Press.

Denny, M. W. and Gaylord, B. (2010). Marine ecomechanics. *Annu. Rev. Mar. Sci.* **2**, 89-114.

Denny, M. W. and Shibata, M. F. (1989). Consequences of surf-zone turbulence for settlement and external fertilization. *Am. Nat.* **134**, 859-889.

Denny, M. W., Dairiki, J. and Distefano, S. (1992). Biological consequences of topography on wave-swept rocky shores: I. Enhancement of external fertilization. *Biol. Bull.* **183**, 220-232.

Denny, M. W., Nelson, E. K. and Mead, K. S. (2002). Revised estimates of the effects of turbulence on fertilization in the purple sea urchin, *Strongylocentrotus purpuratus*. *Biol. Bull.* **203**, 275-277.

Ducasse, L. and Pumir, A. (2008). Intermittent particle distribution in synthetic free-surface turbulent flows. *Phys. Rev. E* **77**, 066304.

Dusenbery, D. B. (2000). Selection for high gamete encounter rates explains the success of male and female mating types. *J. Theor. Biol.* **202**, 1-10.

Dusenbery, D. B. (2002). Ecological models explaining the success of distinctive sperm and eggs (oogamy). *J. Theor. Biol.* **219**, 1-7.

Eckart, C. (1948). An analysis of the stirring and mixing processes in incompressible fluids. *J. Mar. Res.* **7**, 265-275.

Eckhardt, B. and Schumacher, J. (2001). Turbulence and passive scalar transport in a free-slip surface. *Phys. Rev. E* **64**, 16314.

Eckman, J. E. (1996). Closing the larval loop: linking larval ecology to the population dynamics of marine benthic invertebrates. *J. Exp. Mar. Biol. Ecol.* **200**, 207-237.

Edouard, S., Legras, B. and Zeitlin, V. (1996). The effect of dynamical mixing in a simple model of the ozone hole. *J. Geophys. Res. Atmos.* **101**, 16771-16778.

Farley, G. S. and Levitan, D. R. (2001). The role of jelly coats in sperm-egg encounters, fertilization success, and selection on egg size in broadcast spawners. *Am. Nat.* **157**, 626-636.

Ferrier, G., Davies, P. A. and Anderson, J. M. (1996). Remote sensing observations of a vortex street downstream of an obstacle in an estuarine flow. *Int. J. Remote Sens.* **17**, 1-8.

Garrett, C. (1983). On the initial streakiness of a dispersing tracer in two- and three-dimensional turbulence. *Dyn. Atmos. Oceans* **7**, 265-277.

Gaylord, B. (2008). Hydrodynamic context for considering turbulence impacts on external fertilization. *Biol. Bull.* **214**, 315-318.

Giese, A. C. and Pearse, J. S. (1974). *Reproduction of Marine Invertebrates*. New York: Academic Press.

Goldburg, W. I., Cressman, J. R., Vörös, Z., Eckhardt, B. and Schumacher, J. (2001). Turbulence in a free surface. *Phys. Rev. E* **63**, 65303.

Grant, W. D. and Madsen, O. S. (1979). Combined wave and current interaction with a rough bottom. *J. Geophys. Res. Oceans Atmos.* **84**, 1797-1808.

Gray, J. (1955). The movement of sea-urchin spermatozoa. *J. Exp. Biol.* **32**, 775-801.

Guichard, F. and Bourget, E. (1998). Topographic heterogeneity, hydrodynamics, and benthic community structure: a scale-dependent cascade. *Mar. Ecol. Prog. Ser.* **171**, 59-70.

Helgesen, J. K. and Matteson, M. J. (1994). Particle mixing and diffusion in the turbulent wake of a single cylinder. *Aerosol Sci. Technol.* **20**, 111-126.

Hill, P. S. and McCave, I. N. (2001). Suspended particle transport in benthic boundary layers. In *The Benthic Boundary Layer: Transport Processes and Biogeochemistry* (ed. B. P. Boudreau and B. B. Jørgensen), pp. 78-103. New York: Oxford University Press.

Hill, P. S. and Nowell, A. R. M. (1995). Comparison of two models of aggregation in continental-shelf bottom boundary layers. *J. Geophys. Res.* **100**, 22749-22763.

Hill, P. S., Nowell, A. R. M. and Jumars, P. A. (1992). Encounter rate by turbulent shear of particles similar in diameter to the Kolmogorov scale. *J. Mar. Res.* **50**, 643-668.

Hinch, E. J. (1999). Mixing: turbulence and chaos – an introduction. In *Mixing: Chaos and Turbulence* (ed. H. Chaté, E. Villermaux and J.-M. Chomaz), pp. 37-56. New York: Kluwer Academic/Plenum Publishers.

Hodgson, A. N., Le Quesne, W. J. F., Hawkins, S. J. and Bishop, J. D. D. (2007). Factors affecting fertilization success in two species of patellid limpet (Mollusca: Gastropoda) and development of fertilization kinetics models. *Mar. Biol.* **150**, 415-426.

Jackson, G. A. (2012). Seascapes: the world of aquatic organisms as determined by their particulate natures. *J. Exp. Biol.* **215**, 1017-1030.

Jackson, G. A. and Burd, A. B. (1998). Aggregation in the marine environment. *Environ. Sci. Technol.* **32**, 2805-2814.

Jantzen, T. M., de Nys, R. and Havenhand, J. N. (2001). Fertilization success and the effects of sperm chemoattractants on effective egg size in marine invertebrates. *Mar. Biol.* **138**, 1153-1161.

Karolyi, G., Pentek, A., Toroczkai, Z., Tel, T. and Grebogi, C. (1999). Chemical or biological activity in open chaotic flows. *Phys. Rev. E* **59**, 5468-5481.

Kastrinakis, E. G. and Nychas, S. G. (1998). Mixing at high Schmidt numbers in the near wake of a circular cylinder. *Chem. Eng. Sci.* **53**, 3977-3989.

Kumar, S., Gupta, R. and Banerjee, S. (1998). An experimental investigation of the characteristics of free-surface turbulence in channel flow. *Phys. Fluids* **10**, 437.

Larson, R. J. (1992). Riding Langmuir circulations and swimming in circles: a novel form of clustering behavior by the scyphomedusa *Linuche unguiculata*. *Mar. Biol.* **112**, 229-235.

Lauzon-Guay, J. S. and Scheibling, R. E. (2007). Importance of spatial population characteristics on the fertilization rates of sea urchins. *Biol. Bull.* **212**, 195-205.

Levitan, D. R. (1993). The importance of sperm limitation to the evolution of egg size in marine invertebrates. *Am. Nat.* **141**, 517-536.

Levitan, D. R. (1995). The ecology of fertilization in free-spawning invertebrates. In *Ecology of Marine Invertebrate Larvae* (ed. L. McEdward), pp. 123-156. Boca Raton, FL: CRC Press.

Levitan, D. R. (2002). Density-dependent selection on gamete traits in three congeneric sea urchins. *Ecology* **83**, 464-479.

Levitan, D. R. (2005a). The distribution of male and female reproductive success in a broadcast spawning marine invertebrate. *Integr. Comp. Biol.* **45**, 848-855.

Levitan, D. R. (2005b). Sex-specific spawning behavior and its consequences in an external fertilizer. *Am. Nat.* **165**, 682-694.

Levitan, D. R. (2006). The relationship between egg size and fertilization success in broadcast-spawning marine invertebrates. *Integr. Comp. Biol.* **46**, 298-311.

Levitan, D. R. and Young, C. M. (1995). Reproductive success in large populations: empirical measures and theoretical predictions of fertilization in the sea biscuit *Clypeaster rosaceus*. *J. Exp. Mar. Biol. Ecol.* **190**, 221-241.

Levitan, D. R., Sewell, M. A. and Chia, F. (1991). Kinetics of fertilization in the sea urchin *Strongylocentrotus franciscanus*: interaction of gamete dilution, age, and contact time. *Biol. Bull.* **181**, 371-378.

Levitan, D. R., Sewell, M. A. and Chia, F. (1992). How distribution and abundance influence fertilization success in the sea urchin *Strongylocentrotus franciscanus*. *Ecology* **73**, 248-254.

Lewis, D. M. (2003). Planktonic encounter rates in homogeneous isotropic turbulence: the case of predators with limited fields of sensory perception. *J. Theor. Biol.* **222**, 73-97.

Lukaschuk, S., Denissenko, P. and Falkovich, G. (2006). Clustering of floating particles by surface waves. *J. Low Temp. Phys.* **145**, 297-310.
Luttikhuizen, P. C., Honkoop, P. J. C., Drent, J. and van der Meer, J. (2004). A general solution for optimal egg size during external fertilization, extended scope for intermediate optimal egg size and the introduction of Don Ottavio 'tango'. *J. Theor. Biol.* **231**, 333-343.
Marshall, D. J. (2002). *In situ* measures of spawning synchrony and fertilization success in an intertidal, free-spawning invertebrate. *Mar. Ecol. Prog. Ser.* **236**, 113-119.
Maxey, M. R. (1990). On the advection of spherical and non-spherical particles in a non-uniform flow. *Philos. Trans. R. Soc. Lond. A* **333**, 289-307.
McEuen, F. S. (1988). Spawning behaviors of Northeast Pacific sea cucumbers (Holothuroidea, Echinodermata). *Mar. Biol.* **98**, 565-585.
Mead, K. S. and Denny, M. W. (1995). The effects of hydrodynamic shear stress on fertilization and early development of the purple sea urchin *Strongylocentrotus purpuratus*. *Biol. Bull.* **188**, 46-56.
Meidel, S. K. and Yund, P. O. (2001). Egg longevity and time-integrated fertilization in a temperate sea urchin (*Strongylocentrotus droebachiensis*). *Biol. Bull.* **201**, 84-94.
Metaxas, A., Scheibling, R. E. and Young, C. M. (2002). Estimating fertilization success in marine benthic invertebrates: a case study with the tropical sea star *Oreaster reticulatus*. *Mar. Ecol. Prog. Ser.* **226**, 87-101.
Millar, R. B. and Anderson, M. J. (2003). The kinetics of monospermic and polyspermic fertilization in free-spawning marine invertebrates. *J. Theor. Biol.* **224**, 79-85.
Miller, R. L. (1985). Demonstration of sperm chemotaxis in Echinodermata: Asteroidea, Holothuroidea, Ophiuroidea. *J. Exp. Zool.* **234**, 383-414.
Miller, R. L. (1997). Specificity of sperm chemotaxis among Great Barrier Reef shallow-water holothurians and ophiuroids. *J. Exp. Zool.* **279**, 189-200.
Moore, P. and Crimaldi, J. P. (2004). Odor landscapes and animal behavior: tracking odor plumes in different physical worlds. *J. Mar. Syst.* **49**, 55-64.
Moore, S. W. (2003). Scrambled eggs: mechanical forces as ecological factors in early development. *Evol. Dev.* **5**, 61-66.
Niederkorn, T. C. and Ottino, J. M. (1994). Chaotic mixing of shear-thinning fluids. *AIChE J.* **40**, 1782-1793.
Oliver, J. K. and Willis, B. L. (1987). Coral-spawn slicks in the Great Barrier Reef – preliminary observations. *Mar. Biol.* **94**, 521-529.
Ottino, J. M. (1989). *The Kinematics of Mixing: Stretching, Chaos, and Transport*. Cambridge: Cambridge University Press.
Ottino, J. M. (1994). Mixing and chemical reactions – a tutorial. *Chem. Eng. Sci.* **49**, 4005-4027.
Pearson, G. A. and Brawley, S. H. (1996). Reproductive ecology of *Fucus distichus* (Phaeophyceae): an intertidal alga with successful external fertilization. *Mar. Ecol. Prog. Ser.* **143**, 211-223.
Pennington, J. T. (1985). The ecology of fertilization of echinoid eggs: the consequences of sperm dilution, adult aggregation, and synchronous spawning. *Biol. Bull.* **169**, 417-430.
Picken, G. B. and Allan, D. (1983). Invertebrate reproduction: unique limpet spawning behavior. *Nature* **305**, 472.
Podolsky, R. D. (2001). Evolution of egg target size: an analysis of selection on correlated characters. *Evolution* **55**, 2470-2478.
Podolsky, R. D. (2002). Fertilization ecology of egg coats: physical versus chemical contributions to fertilization success of free-spawned eggs. *J. Exp. Biol.* **205**, 1657-1668.
Pope, S. B. (2000). *Turbulent Flows*. Cambridge: Cambridge University Press.
Reade, W. C. and Collins, L. R. (2000). Effect of preferential concentration on turbulent collision rates. *Phys. Fluids* **12**, 2530.
Rehab, H., Antonia, R. A. and Djenidi, L. (2001). Streamwise evolution of a high-Schmidt-number passive scalar in a turbulent plane wake. *Exp. Fluids* **31**, 186-192.
Reidenbach, M. A., Koseff, J. R., Monismith, S. G., Steinbuck, J. V. and Genin, A. (2006). The effects of waves and morphology on mass transfer within branched reef corals. *Limnol. Oceanogr.* **51**, 1134-1141.
Reigada, R., Sagues, F. and Sancho, J. M. (2001). Inertial effects on reactive particles advected by turbulence. *Phys. Rev. E* **64**, 026307.
Richardson, L. F. (1926). Atmospheric diffusion shown on a distance-neighbour graph. *Proc. R. Soc. Lond. A* **110**, 709-737.
Riffell, J. A. and Zimmer, R. K. (2007). Sex and flow: the consequences of fluid shear for sperm–egg interactions. *J. Exp. Biol.* **210**, 3644-3660.
Rothschild, B. J. and Osborn, T. R. (1988). Small-scale turbulence and plankton contact rates. *J. Plankton Res.* **10**, 465-474.
Sanford, L. P. (1997). Turbulent mixing in experimental ecosystem studies. *Mar. Ecol. Prog. Ser.* **161**, 265-293.
Schumacher, J. and Eckhardt, B. (2002). Clustering dynamics of Lagrangian tracers in free-surface flows. *Phys. Rev. E* **66**, 017303.
Shen, L., Zhang, X., Yue, D. K. P. and Triantafyllou, G. S. (1999). The surface layer for free-surface turbulent flows. *J. Fluid Mech.* **386**, 167-212.
Singh, P. and Joseph, D. D. (2005). Fluid dynamics of floating particles. *J. Fluid Mech.* **530**, 31-80.
Sokolov, I. M. (1999). Two-particle dispersion by correlated random velocity fields. *Phys. Rev. E* **60**, 5528.
Soltys, M. A. and Crimaldi, J. P. (2010). Scalar interactions between parallel jets measured using a two-channel PLIF technique. *Exp. Fluids* **50**, 1625-1632.
Squires, K. D. and Eaton, J. K. (1991). Preferential concentration of particles by turbulence. *Phys. Fluids A* **3**, 1169.
Squires, K. D. and Yamazaki, H. (1995). Preferential concentration of marine particles in isotropic turbulence. *Deep Sea Res. Part I Oceanogr. Res. Pap.* **42**, 1989-2004.
Styan, C. A. (1998). Polyspermy, egg size, and the fertilization kinetics of free-spawning marine invertebrates. *Am. Nat.* **152**, 290-297.
Styan, C. A. and Butler, A. J. (2000). Fitting fertilisation kinetics models for free-spawning marine invertebrates. *Mar. Biol.* **137**, 943-951.
Styan, C. A., Byrne, M. and Franke, E. (2005). Evolution of egg size and fertilisation efficiency in sea stars: large eggs are not fertilised more readily than small eggs in the genus *Patiriella* (Echinodermata: Asteroidea). *Mar. Biol.* **147**, 235-242.
Tang, L., Wen, F., Yang, Y., Crowe, C. T., Chung, J. N. and Troutt, T. R. (1992). Self-organizing particle dispersion mechanism in a plane wake. *Phys. Fluids A* **4**, 2244-2251.
Thomas, F. I. M. (1994a). Physical properties of gametes in three sea urchin species. *J. Exp. Biol.* **194**, 263-284.
Thomas, F. I. M. (1994b). Transport and mixing of gametes in three free-spawning polychaete annelids, *Phragmatopoma californica* (Fewkes), *Sabellaria cementarium* (Moore), and *Schizobranchia insignis* (Bush). *J. Exp. Mar. Biol. Ecol.* **179**, 11-27.
Thorpe, S. A. (2004). Langmuir circulation. *Annu. Rev. Fluid Mech.* **36**, 55-79.
Toroczkai, Z., Károlyi, G., Péntek, Tél, T. and Grebogi, C. (1998). Advection of active particles in open chaotic flows. *Phys. Rev. Lett.* **80**, 500-503.
Vogel, H., Czihak, G., Chang, P. and Wolf, W. (1982). Fertilization kinetics of sea urchin eggs. *Math. Biosci.* **58**, 189-216.
Warhaft, Z. (2000). Passive scalars in turbulent flows. *Annu. Rev. Fluid Mech.* **32**, 203-240.
Yund, P. O. (2000). How severe is sperm limitation in natural populations of marine free-spawners? *Trends Ecol. Evol.* **15**, 10-13.
Yund, P. O. and Meidel, S. K. (2003). Sea urchin spawning in benthic boundary layers: are eggs fertilized before advecting away from females? *Limnol. Oceanogr.* **48**, 795-801.